Practical iterative image reconstruction in digital breast tomosynthesis by non-convex TpV optimization

Emil Y Sidky[a], Ingrid Reiser[a], Robert M. Nishikawa[a], Xiaochuan Pan[a], Rick Chartrand[b], Daniel B Kopans[c] and Richard H Moore[c]

[a]Department of Radiology, The University of Chicago, Chicago, IL
[b]Los Alamos National Laboratory, Los Alamos, NM
[c]Massachusetts General Hospital, Boston, MA

ABSTRACT

Digital breast tomosynthesis (DBT) is a rapidly developing imaging modality that gives some tomographic information for breast cancer screening. The effectiveness of standard mammography can be limited by the presence of overlapping structures in the breast. A DBT scan, consisting of a limited number of views covering a limited arc projecting the breast onto a fixed flat-panel detector, involves only a small modification of digital mammography, yet DBT yields breast image slices with reduced interference from overlapping breast tissues. We have recently developed an iterative image reconstruction algorithm for DBT based on image total variation (TV) minimization that improves on EM in that the resulting images have fewer artifacts and there is no need for additional regularization. In this abstract, we present the total p-norm variation (TpV) image reconstruction algorithm. TpV has the advantages of our previous TV algorithm, while improving substantially on the efficiency. Results for the TpV on clinical data are shown and compared with EM.

Keywords: iterative reconstruction, non-convex optimization, tomosynthesis

1. INTRODUCTION

Digital breast tomosynthesis (DBT)[1] is an emerging modality that produces three-dimensional breast images. Screening mammography suffers from the limitation that the complex 3D breast structure is projected into a plane. Lesions can be obscured by overlaying tissue structures which could cause a false negative, or dense overlapping tissue can mimic lesions, leading to an unnecessary recall of a patient. In DBT, lesion conspicuity is improved, which could potentially lead to earlier cancer detection and a more accurate diagnosis.

In tomosynthesis, a volume image is created from a sequence of projection views acquired over a limited arc. Reconstruction from this data is challenging because the data is inherently incomplete. One-shot algorithms such as filtered back-projection (FBP) have been developed for DBT image reconstruction. Though efficient, they tend to yield conspicuous artifacts. Iterative algorithms such as expectation-maximization (EM) have also been employed with DBT. Such algorithms sacrifice efficiency, but yield images with fewer artifacts. An additional drawback for EM, however, is that in general some form of regularization is needed which tends to reduce resolving power necessary for calcification detection.

Mathematically, this reconstruction problem can be thought of as an underdetermined linear system. There will not be a unique solution to this linear system even under conditions of ideal data. However, the solution can be narrowed down by making assumptions on the image. If the image is sparse in some representation, then a sparse solution can be found by minimizing the L_0 norm of the image, while imposing a constraint that the image agrees with the measured projection data to some extent.[2,3] While minimization of the L_0 norm is not practical, minimization of the L_1 norm is equivalent under certain conditions. L_1 norm minimization is a convex optimization problem for which there exist practical algorithms. One could further minimize the L_p norm where $0 < p < 1$.[4] There may be an advantage in the presence of data inconsistencies and noise.

We have previously developed an algorithm that is effective at reconstructing tomosynthesis images by finding the image with the minimum total variation (TV) under the constraint that the image agrees with the projection data up to a specified data tolerance. The total variation is the L_1 norm of the image gradient magnitude.[5]

The purpose of this work is to investigate image reconstruction through miminizing the L_p norm (p=0.8) of the image gradient magnitude (TpV), rather than the L_1 norm, under the constraint that the image agrees with the projection data to within a set tolerance. The effectiveness of this new algorithm is demonstrated by comparing patient data reconstructed with several iterative algorithms, namely POCS, TV, TpV, and EM. Further, we will show the behaviour of each algorithm for truncated iterations.

In section 2, an overview of L_p norm minimization will be given, and section 3 will describe the imaging system used to acquire the patient data. In section 4, we sill show examples of clinical patient images reconstructed with each algorithm.

2. METHODS

For the TpV algorithm the optimization problem we seek to solve is:

$$\vec{f}^* = \text{argmin } \|\nabla f\|_{TpV} \text{ subject to } \|\mathbf{M}\vec{f} - \vec{g}\| \leq \epsilon. \tag{1}$$

The vector $\vec{f}$ denotes the pixel/voxel representation of the image; $\vec{g}$ is the discrete set of projection data; and $\mathbf{M}$ is the system matrix, which for the examples shown below is the ray-driven projection of the image matrix. The quantity $\|\nabla f\|_p$ is the p-norm of the image gradient magnitude, and for 3D images we define it by

$$\|\nabla f\|_p^p \equiv \sum_{i,j,k} \left(\sqrt{(f_{i,j,k} - f_{i-1,j,k})^2 + (f_{i,j,k} - f_{i,j-1,k})^2 + (f_{i,j,k} - f_{i,j,k-1})^2} \right)^p . \tag{2}$$

The optimization problem specified by Eqs. (1) and (2) depends on two parameters ϵ and p. When $p = 1$, TpV optimization reduces to TV optimization. The data constraint in Eq. (1) allows for the fact that the data $\vec{g}$ may be inconsistent, i.e. there may be no image $\vec{f}$ that satisfies $\mathbf{M}\vec{f} = \vec{g}$. Such inconsistency can occur when the projector model does not coincide with the actual projection or when the data contain noise. In general the minimum data tolerance $\epsilon_{\min}$, the minimum ϵ such that there exists an $\vec{f}$ satisfying $\|\mathbf{M}\vec{f} - \vec{g}\| \leq \epsilon$, is larger than zero. As ϵ increases, images with smaller TpV are obtained. In general, the standard TV norm will not identify the image with the sparsest image gradient, here, because the image constraint is ellipsoidal, not linear. Reducing p, however, brings Eq. (1) closer to the ideal $p = 0$ case that does yield the sparse image gradient solution. When the underlying image function satisfies the assumption of image gradient sparseness, the reduction of p to values below $p = 1$ can improve the accuracy of the image reconstruction.

In our implementation, POCS (projection onto convex sets) is used to enforce data consistency as well as pixel value constraints:

$$(M\vec{f} - \vec{g})^2 < \epsilon^2 \text{ and } f_{max} > \vec{f} \geq 0 \tag{3}$$

The ML-EM algorithm shown is based on the update equation

$$\vec{f}_{k+1} = \vec{f}_k \frac{1}{s} M^+ \{ \frac{\vec{g}}{M\vec{f}_k} \} \tag{4}$$

where M and M^+ are the forward and backprojection operators, $s = \sum M$, and $\frac{\vec{g}}{M\vec{f}_k}$ indicates a division between the vector elements. Note that the data $\vec{g}$ is not Poisson-distributed because of the indirect detector used to acquire the projection views. The EM algorithm is implicitly regularized because an unmatched projector-backprojector pair is used, i.e., the projector is ray-driven, while the backprojector is voxel-driven.

3. MATERIALS

The clinical data was acquired at the Massachusetts General Hospital in Boston, MA. Patient data was acquired under IRB approval following informed consent. Patients were imaged by tomosynthesis prior to undergoing biopsy. The tomosynthesis scan configuration was such that the x-ray source covered an arc of 50 degrees while acquiring 11 projection views in step-and-shoot mode. The detector was stationary during the scan. Detector pixel size was 100 microns. The source pivoting point was located at 23.7 cm above the detector surface, and the gantry rotated on an arc with 41.2 cm radius. Voxel size was 100 microns x 100 microns x 1mm.[1]

Two patient data sets were selected. One dataset contained a mass lesion, the other contained a micro-calcification cluster.

4. RESULTS

In the following, the in-focus slice of a mass lesion is shown, reconstructed with POCS, TV, TpV, and EM at 1, 5, and 10 iterations. Note that the projection data for this case is contaminated with horizontal lines that become apparent in all reconstructions. The stripes are somewhat less apparent for the EM reconstruction, which may be because the EM slice has a smoother appearance overall. For all data sets and number of iterations, POCS is shown as a reference since it is part of the TV and TpV algorithms.

(a) POCS (b) TV (c) TpV (d) EM

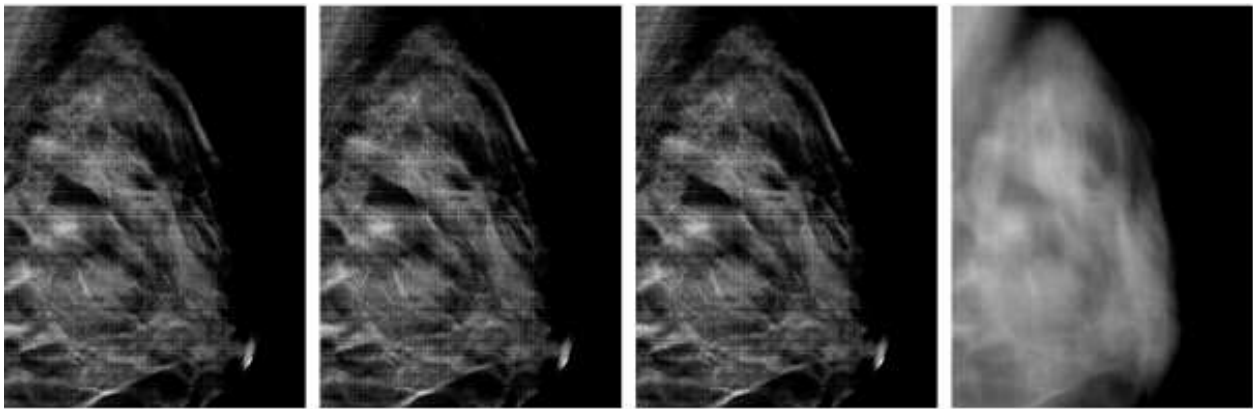

Figure 1. Reconstruction of a breast volume containing a mass lesion, shown after one iteration. (a) POCS, (b) TV, (c) TpV, (d) EM. The display range for (a)-(c) is [0.4,0.6], while it is [0.37,0.52] for (d).

(a) POCS (b) TV (c) TpV (d) EM

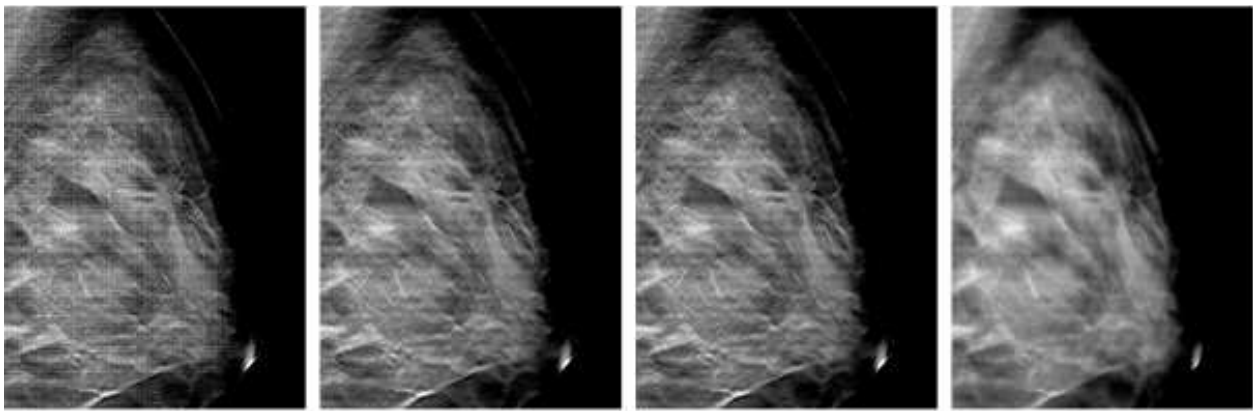

Figure 2. Same as Fig. 1, after 5 iterations.

(a) POCS (b) TV (c) TpV (d) EM

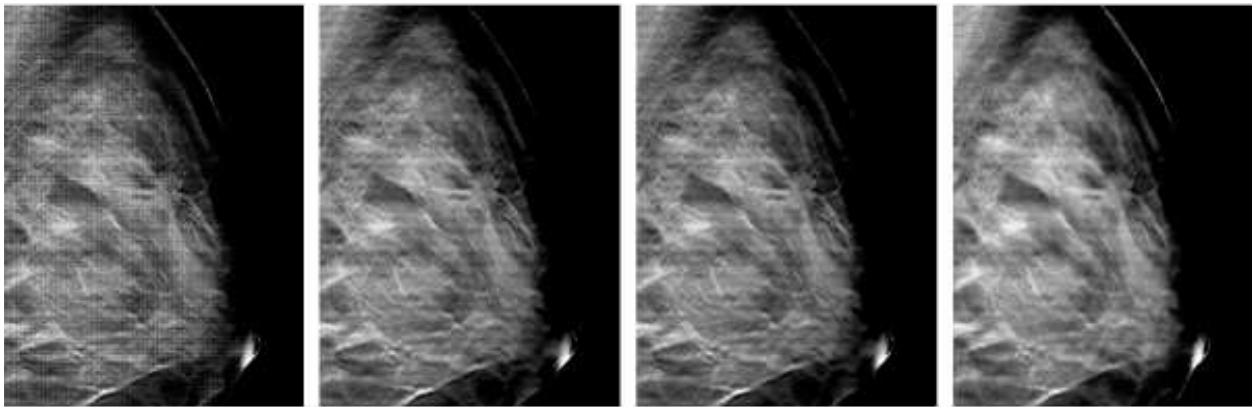

Figure 3. Same as Fig. 1, after 10 iterations.

The next set of images show the in-focus plane of a microcalcification cluster. Microcalcifications appear much clearer in both TV and TpV than EM, for all iterations.

5. DISCUSSION

The images shown for POCS are not representative of POCS as a reconstruction algorithm, because no regularization was used. However, unregularized POCS is shown here because it is the base part of the TV and TpV algorithms and the comparison highlights the effects of the TV and TpV gradient descent. For both TV and TpV, it is striking that image features become apparent after a single iteration, while it requires several iterations of the EM algorithm to achieve this. For the mass lesions, after 10 iterations, slightly more structure is discernible in the total variation-based algorithms. The difference in appeareance of the microcalcification cluster is striking, a much larger number of individual calcifications can be seen in the total variation minimization reconstructed images.

In this study, we compared algorithm performance using patient data. While visual assessment of image quality is by no means a quantitative evaluation, it is important to demonstrate that each algorithm is capable of reconstructing images from actual data. While comparisons based on phantom data are more

(a) POCS (b) TV (c) TpV (d) EM

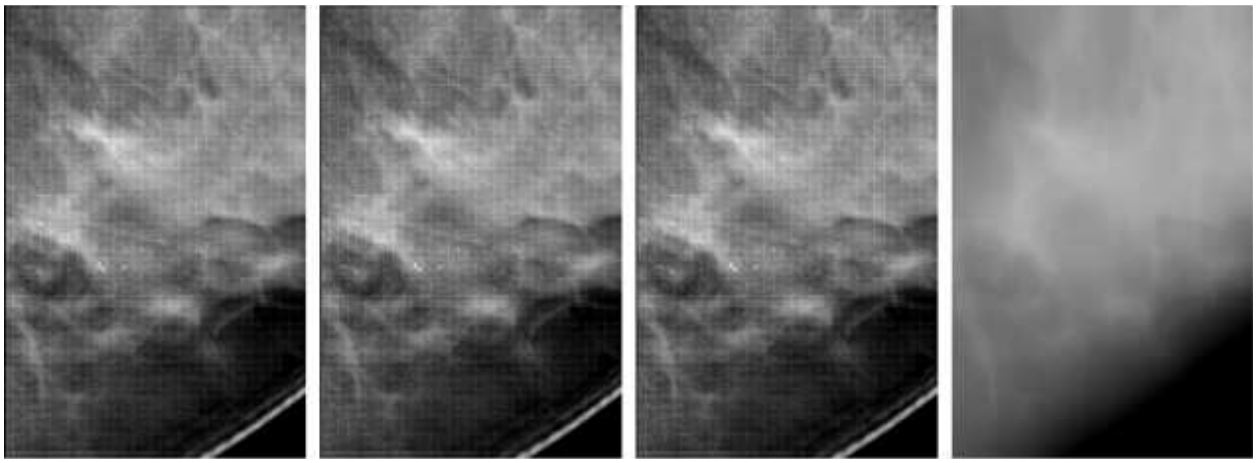

Figure 4. Reconstruction of a breast volume containing a microcalcification cluster, shown after one iteration. (a) POCS, (b) TV, (c) TpV, (d) EM. The display range for (a)-(c) is [0.3,0.6], while it is [0.3,0.55] for (d).

(a) POCS (b) TV (c) TpV (d) EM

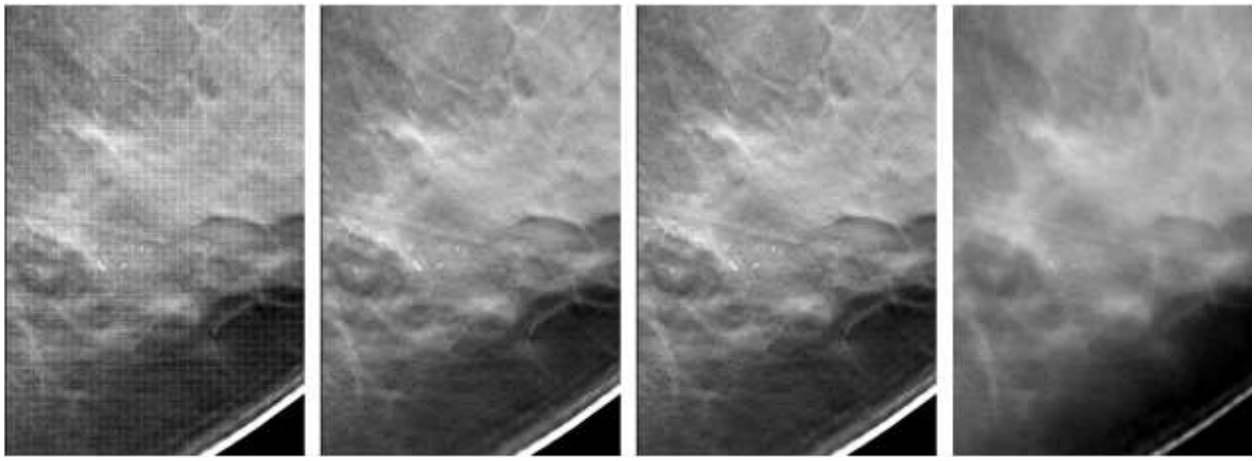

Figure 5. Same as Fig. 4, after 5 iterations.

quatitative, they represent ideal data to some degree, since some physical factors may not be included in data models, for instance, few data models account for patient motion and calibration errors.

6. CONCLUSION

In conclusion, we have developed practical TV and TpV algorithms for reconstruction of tomosynthesis images. Visually, the image quality of clinical images is comparable to ML-EM, in particular, for masses. However, TV and TpV minimization may have advantages when imaging microcalcification clusters.

ACKNOWLEDGMENTS

This work was funded in part by the National Cancer Institute grants R33 CA109963 and K01 EB003913 (EYS). RM Nishikawa is a shareholder in Hologic, Inc. and receives both research funds and royalties from

(a) POCS (b) TV (c) TpV (d) EM

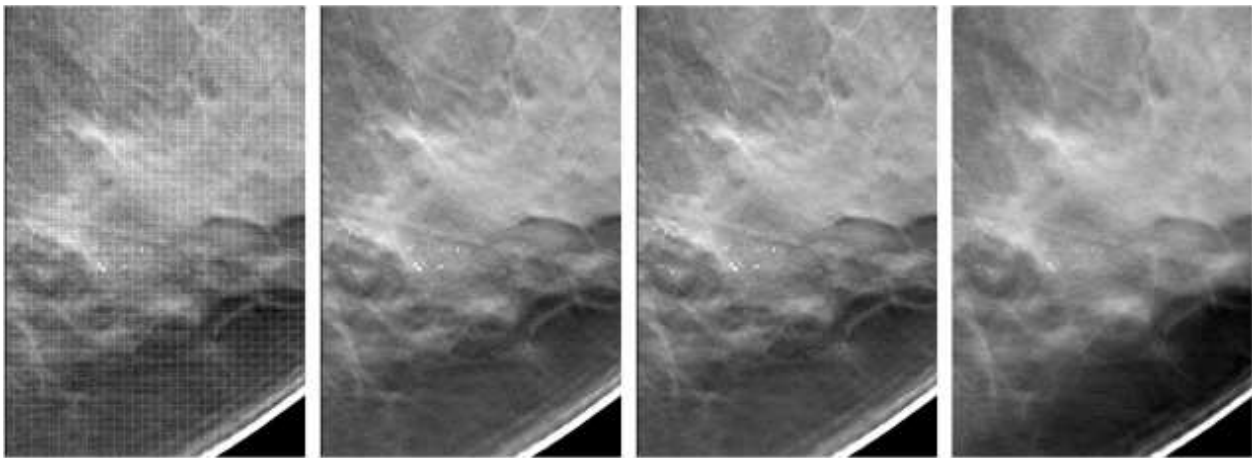

Figure 6. Same as Fig. 4, after 10 iterations.

Hologic. Inc. RM Nishikawa is also on the scientific advisory board of Dexela Ltd. DB Kopans is a patent holder for the technique of breast tomosynthesis and the Breast Imaging Division at the Massachusetts General Hospital received some research support from the General Electric Company.

REFERENCES

1. T. Wu, A. Stewart, M. Stanton, T. McCauley, W. Phillips, D. B. Kopans, R. H. Moore, J. W. Eberhard, B. Opsahl-Ong, L. Niklason, and M. B. Williams, "Tomographic mammography using a limited number of low-dose cone-beam projection images," *Med. Phys.* **30**, pp. 365–380, 2003.
2. E. J. Candès, J. K. Romberg, and T. Tao, "Stable signal recovery from incomplete and inaccurate measurem ents," *Commun. Pure Appl. Math.* **59**, pp. 1207–1223, 2006.
3. E. J. Candès, J. Romberg, and T. Tao, "Robust uncertainty principles: Exact signal reconstruction fro m highly incomplete frequency information," *IEEE Trans. Inf. Theory* **52**, 2006.
4. R. Chartrand, "Exact reconstruction of sparse signals via nonconvex minimizat ion," *IEEE Signal Process. Lett.* **14**, pp. 707–710, 2007.
5. E. Y. Sidky, C.-M. Kao, and X. Pan, "Accurate image reconstruction from few-views and limited-angle data in divergent-beam CT," *J. X-ray Sci. Tech.* **14**, pp. 119–139, 2006.